A mechanism for sustained groundwater pressure changes induced by distant earthquakes

Emily E. Brodsky,[1] Evelyn Roeloffs,[2] Douglas Woodcock,[3] Ivan Gall,[4] and Michael Manga[5]

Received 25 November 2002; revised 8 March 2003; accepted 3 April 2003; published 22 August 2003.

[1] Large, sustained well water level changes (>10 cm) in response to distant (more than hundreds of kilometers) earthquakes have proven enigmatic for over 30 years. Here we use high sampling rates at a well near Grants Pass, Oregon, to perform the first simultaneous analysis of both the dynamic response of water level and sustained changes, or steps. We observe a factor of 40 increase in the ratio of water level amplitude to seismic wave ground velocity during a sudden coseismic step. On the basis of this observation we propose a new model for coseismic pore pressure steps in which a temporary barrier deposited by groundwater flow is entrained and removed by the more rapid flow induced by the seismic waves. In hydrothermal areas, this mechanism could lead to 4×10^{-2} MPa pressure changes and triggered seismicity. *INDEX TERMS:* 1829 Hydrology: Groundwater hydrology; 7209 Seismology: Earthquake dynamics and mechanics; 7212 Seismology: Earthquake ground motions and engineering; 7260 Seismology: Theory and modeling; 7294 Seismology: Instruments and techniques; *KEYWORDS:* earthquakes, triggering, time-dependent hydrology, fractures

Citation: Brodsky, E. E., E. Roeloffs, D. Woodcock, I. Gall, and M. Manga, A mechanism for sustained groundwater pressure changes induced by distant earthquakes, *J. Geophys. Res.*, *108*(B8), 2390, doi:10.1029/2002JB002321, 2003.

1. Introduction

[2] Earthquakes can produce sustained water level changes in certain distant wells [*Coble*, 1965; *Bower and Heaton*, 1978; *Matsumoto*, 1992; *Roeloffs*, 1998; *King et al.*, 1999] that are often orders of magnitude larger than can be explained by static stress changes [*Bower and Heaton*, 1978]. Many researchers suggest that seismic waves interacting with aquifers produce the sustained changes in pore pressure, or steps, hundreds of kilometers from an earthquake [*Bower and Heaton*, 1978; *Roeloffs*, 1998; *King et al.*, 1999]. The redistribution of pore pressure can generate crustal deformation [*Johnston et al.*, 1995] and perhaps even trigger seismicity [*Hill et al.*, 1993; *Brodsky et al.*, 2000; *U.S. Geological Survey* (USGS), 2000]. However, the mechanism by which small cyclic stresses induce persistent pore pressure changes has remained uncertain.

[3] Here we constrain the mechanism for coseismic steps in a well near Grants Pass, Oregon, by using both high sample rate water level data from the well and seismic data from the broadband Berkeley Digital Seismic Network station Yreka Blue Horn Mine (YBH) in Yreka, California (Figure 1). The water level in a well penetrating a confined aquifer is a manometer measuring the pore pressure at a point. During 1993–2001, several seismic water level oscillations and two coseismic steps were recorded digitally. The 1 September 1994 M_w = 7.2 Petrolia, California (epicentral distance Δ = 2.71°), earthquake generated a 15 cm decrease in water level over 2.5 days, and the 30 September 1999 M_w = 7.4 Oaxaca, Mexico (Δ = 34.65°) earthquake generated an immediate 11 cm decrease in water level. We show that (1) the coseismic steps are related to the passage of seismic waves, (2) the amplitude of the water level oscillations relative to the seismic ground velocity increased abruptly at the time of the step induced by the Oaxaca earthquake, and (3) gradual water level steps are consistent with pore pressure changes diffusing to the well from within the aquifer. These observations motivate a new model for distant water level changes. Seismic waves remove a temporary barrier of sediment or solid precipitate resulting in both an increase in the seismic wave amplification and a persistent water level change. We then test the model with a new observation during the 3 November 2002 M_w = 7.9 Alaska earthquake.

2. Observations

[4] The 91.4 m deep NVIP-3 well near Grants Pass, Oregon, has been monitored continuously since 1984 [*Woodcock and Roeloffs*, 1996]. The well is drilled into a fractured granodiorite confined aquifer and a float measures the water level. The chart recorder installed in 1984 was replaced in November 1993 with a digital data logger recording at 1.7×10^{-3} or 1.1×10^{-3} Hz. If the water level changed more than 0.6 mm, the sampling rate increased

[1]Department of Earth and Space Sciences, University of California, Los Angeles, California, USA.
[2]U.S. Geological Survey, Vancouver, Washington, USA.
[3]Oregon Water Resources Department, Salem, Oregon, USA.
[4]Oregon Water Resources Department, Grants Pass, Oregon, USA.
[5]Department of Earth and Planetary Sciences, University of California, Berkeley, California, USA.

0148-0227/03/2002JB002321$09.00

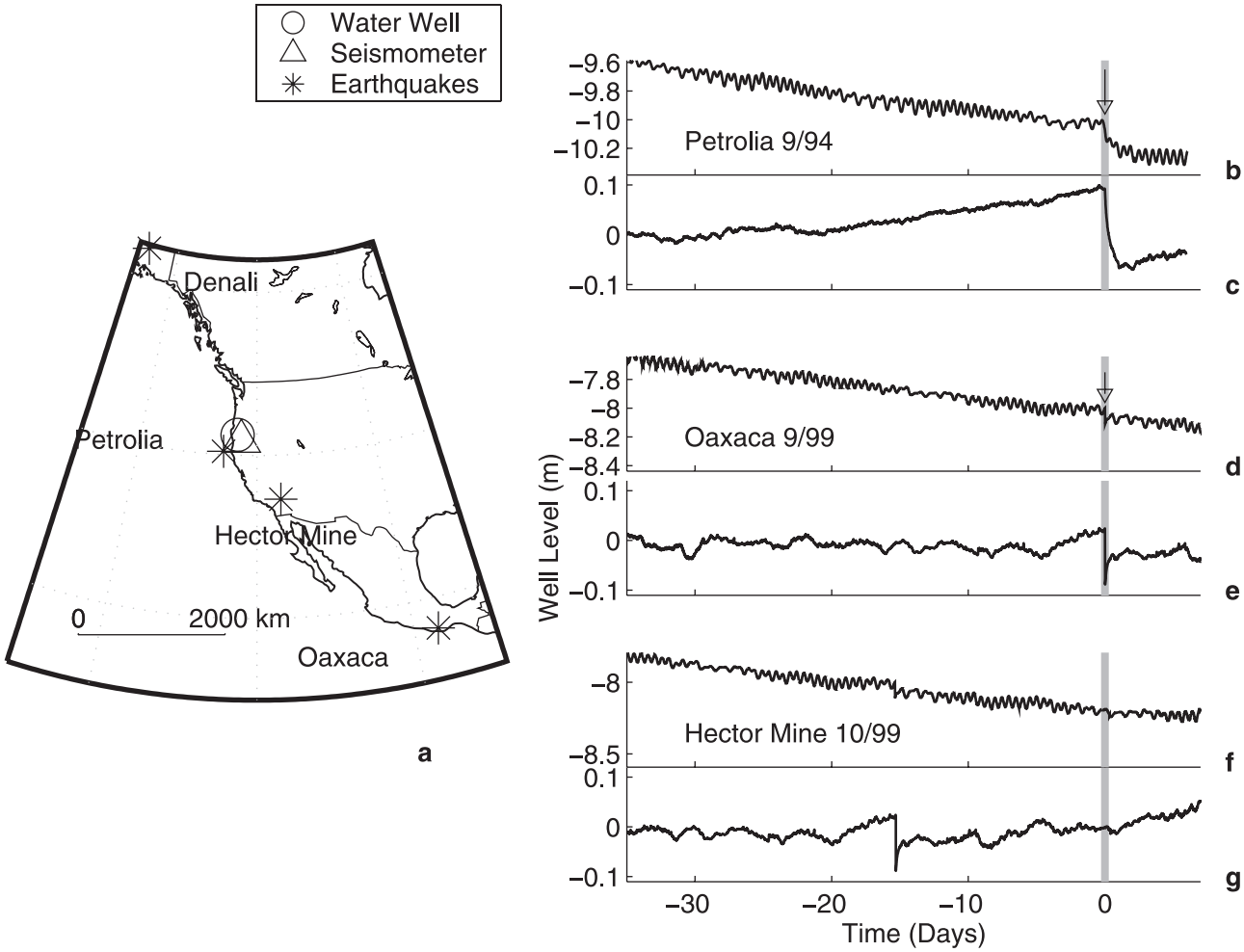

Figure 1. Coseismic water level steps. (a) Map of sites and earthquakes discussed. The distance between the seismometer (YBH) and the well (NVIP-3) is 101 km. (b) Raw well level for Petrolia earthquake. The Petrolia earthquake origin time (time 0) is shaded. The step is marked by an arrow. (c) Well level for Petrolia earthquake with tides, barometric effects and linear trend removed. (d) Same as Figure 1b for Oaxaca. (e) Same as Figure 1c for Oaxaca with the arrow and the shading indicating the Oaxaca earthquake origin time. (f) Same as Figure 1b for Hector Mine with the arrow and the shading indicating the Hector Mine earthquake origin time. No step was observed during this earthquake. The step at −15 days is the Oaxaca earthquake. (g) Same as Figure 1c for Hector Mine. Water well data for Denali are given in Figure 7.

up to a maximum of 1 Hz. In October 1998 a pressure transducer was added sampling at 1.7×10^{-3} Hz. Since March 2001, 1 Hz data from both the float and the transducer have been collected to verify that no instrumental delay is introduced by the float. The well geometry and hydrological properties are given in Table 1. The dynamic response cannot be modeled for the eight earthquake-related water level drops before 1994 [*Woodcock and Roeloffs*, 1996] because the chart records lack sufficient resolution.

[5] Below we first discuss the hydrological and seismological observations pertaining to the oscillatory response of the well in the seismic frequency band (0.02–0.2 Hz). We then present direct observations of steps in water level.

2.1. Oscillatory Well Response to Shaking

[6] During 1993–2001, several earthquakes produced ground shaking on the order of mm s^{-1} at the site and

Table 1. Well Parameters

Variable	Value
Well bore radius r_w	0.06 m
Water column height H	82.8 ± 1.2 m
Tidal response[a] Γ	2.6 ± 0.1 m μstrain^{-1}
Poisson's ratio ν	0.25
Matrix[b] specific storage[c] S_s	4×10^{-7} m^{-1}
Matrix[b] hydraulic conductivity K	6.8×10^{-8} m s^{-1}
Fracture length L	130 m
Phase velocity c	3.7 ± 0.4 km s^{-1}

[a]Observed amplitude of M_2 tidal constituent from 1993–2001 data divided by the theoretical dilatation.

[b]The granodiorite wall rock is the matrix.

[c]Specific storage derived from tidal response following the poroelastic calculation of *Hsieh et al.* [1988]. The upper bound on S_s is $1/\Gamma$ which applies when the rock grains are incompressible. The maximum S_s consistent with the tidal data is used here as it results in physically plausible fracture dimensions [*Hsieh et al.*, 1988]. The maximum value of S_s that meets the tidal constraints is adopted because (1) it is a typical value of crystalline rocks and (2) the resulting fracture size is physically plausible.

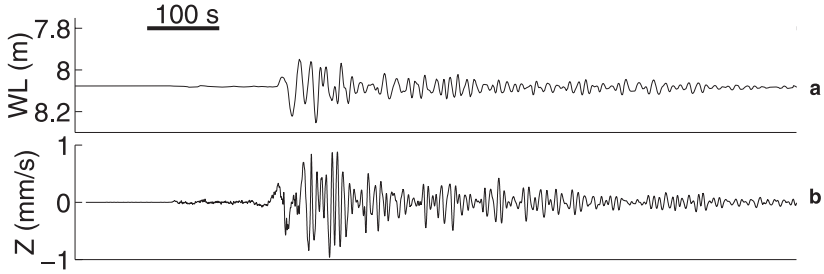

Figure 2. M_w = 7.1 16 October 1999 Hector Mine (Δ = 9.66°) earthquake water well response and seismogram. (a) Water level response at NVIP-3. (b) Vertical component of seismogram recorded at YBH. *Y* axis scales are the same as in Figures 4a and 4b.

water well level oscillations with amplitudes ~10 cm. These large responses imply a large amplification in the well-aquifer system (Figure 2). The water level displacement in the well measures the head change in the aquifer induced by the strain of the seismic waves. Hydraulic head h is defined as $h \equiv p/\rho g - z$, where p is the pore pressure, ρ is the density of water, g is gravitational acceleration, and z is the elevation. For waves in an elastic medium, strain is proportional to particle velocity [e.g., *Love*, 1927, equation XIII.17]. Therefore the amplification of the seismic waves in the well is measured by the ratio χ of the amplitude of the water level oscillations to the particle velocity in the seismic waves. The units of χ are m/(m/s).

[7] The amplification factor χ is computed by dividing the observed well spectra from NVIP-3 by the seismically observed vertical ground velocity spectra from YBH for the records (Figure 3b). Amplitude corrections are applied to the seismograms to account for differences in geometric spreading and radiation pattern between YBH and the well. These corrections are small (<15%) for all of the events discussed in this paper. A 2002 seismic installation showed that both YBH and NVIP-3 are hard rock sites and no site or

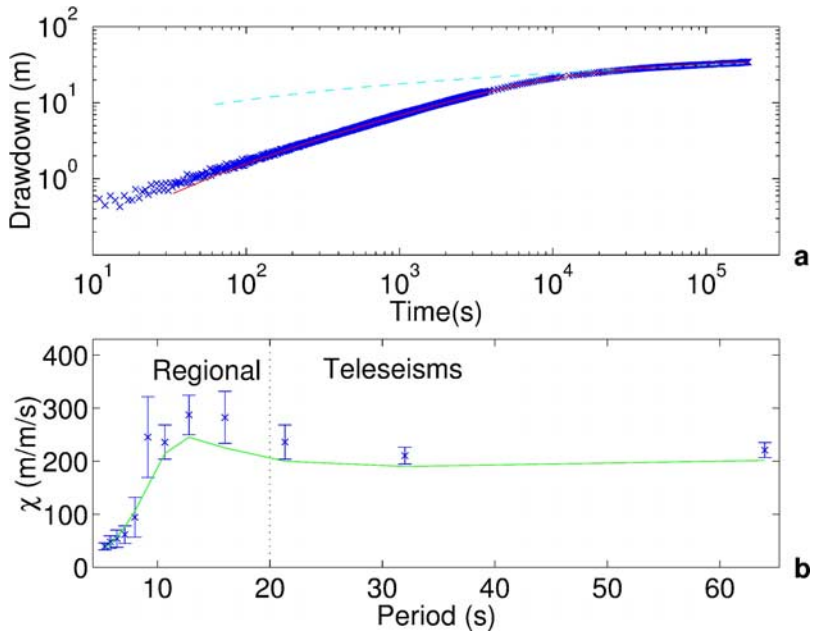

Figure 3. Fits to determine hydraulic conductivity K and fracture length L. (a) Pumping test data (crosses) and best fit model (red line) from equation (2). The drawdown was monitored both manually and by a pressure transducer during a pumping test in November 2001. Data are identical to a November 1981 test. For reference, the dashed line is the best fit standard Theis curve ($K = 8.7 \times 10^{-7}$ m s^{-1}, uncased length 40 m) for the known S_s (Table 1) [*Freeze and Cherry*, 1979]. Pumping test data <10 s are not modeled as there is a transient from turning on the pump. (b) Seismic response data (crosses with error bars) and best fit model (line) from equation (3). The seismic response is determined based on regional earthquakes for periods <20 s and teleseisms for periods >20 s since the seismic waves only have significant signal in these frequency bands. The regional earthquakes used in order of the distance from the well are 1 September 1994 M_w = 7.2 Petrolia, California; 28 February 2001 M_w = 6.8 Nisqually, Washington; 17 January 1994 M_w = 6.7 Northridge, California; 16 October 1999 M_w = 7.1 Hector Mine, California. The teleseisms are 13 January 2001 M_w = 7.7 El Salvador; 4 October 1994 M_w = 8.3 Kuriles and 26 January 2001 M_w = 7.9 Bhuj, India.

soil correction is necessary. Regional earthquakes generate relatively high-frequency signals (>0.05 Hz) while teleseismic waves have lower frequencies. We use the regional events to determine the high-frequency χ and the teleseismic events for the low-frequency χ (Figure 3b). During four regional earthquakes the average observed value of the amplification factor χ is 280 m/(m/s) at 0.06 Hz with a standard deviation of 49 m/(m/s).

[8] The large value of χ quantifies the large amplification in the well and is primarily determined by the small specific storage S_s. Specific storage is defined as the volume of fluid a unit volume of aquifer releases under a unit decrease in head. The definition can be shown to be equivalent to

$$S_s = \rho g(\alpha + \phi\beta), \tag{1}$$

where α and β are the compressibility of the aquifer and fluid, respectively, and ϕ is the porosity [*Freeze and Cherry*, 1979]. Small S_s, indicative of low porosity, is expected for crystalline rock. The small strains of the Earth tides ($\sim 10^{-7}$) which produce large amplitude signals (>6 cm) in the well (Figures 1b, 1d, and 1f) constrain S_s (Table 1). The hydraulic conductivity and local structure also affect χ. The flow through the porous medium and the resonance of the water column in the well both introduce a frequency dependence as discussed below.

[9] We use a pumping test to constrain the geometry of the aquifer near the well. Water was pumped from the well at a rate of 20 GPM (20 GPM = 1.26×10^{-3} m^3 s^{-1}) for 52 hours (1 sample per 10 min or 1 sample per 15 min, respectively). Figure 3 shows that the form of the drawdown curve is well modeled by flow through a single, infinitesimally thin square planar fracture embedded in an unbounded, homogeneous and isotropic confined aquifer. Flux is constant over the surface area of the fracture. The solution for the drawdown curve in this geometry can be derived by integrating point sources or using the Green's function method of *Gringarten and Ramey* [1973] to derive

$$h(t) - h(t=0) = \frac{1}{S_s}\int_0^t \frac{Q(\tau)}{L^2}\frac{1}{2\sqrt{\pi K(t-\tau)/S_s}} \cdot \left(\operatorname{erf}\frac{L}{4\sqrt{K(t-\tau)/S_s}}\right)^2 d\tau, \tag{2}$$

where $h(t)$ is the head in the well, $Q(t)$ is the volumetric withdrawal rate, K is the hydraulic conductivity, and L is the fracture length. The relatively small-radius well intersects and samples the fracture but has no effect on the modeled flow. The shape of both the pumping test curve and the seismic wave response are well-fit by a single fracture model (Figure 3). A simpler, cylindrical flow model (Theis solution) does not fit the data. The geometry is also consistent with the drilling log which recorded a marked increase in flow in the final 2 m of the well. Note that the slope of $\sim$1/2 at early times on the log-log drawdown curve precludes significant storage of water in the fracture and is consistent with the small fracture aperture ($\sim$1 mm) used in the mechanism discussion below.

[10] The linearized response function of the well to seismic waves is calculated following the method of *Cooper et al.* [1965] with the geometry modified to be consistent with the pumping test data in Figure 3. *Cooper et al.* [1965] assumed cylindrical flow into the well; we assume strictly linear flow into the fracture that intersects the well. The pore pressure changes in the aquifer are assumed to be proportional to the dilatational strain of the seismic waves. The most significant dilatation is generated by the Rayleigh wave, rather than the body waves; therefore we only consider the Rayleigh waves as sources of pressure oscillations. The flow directly into the well is assumed negligible because the surface area of the fracture is much greater than the well. The amplification $\chi(f)$ is

$$\chi(f) = A(\nu, c)\Gamma\left|1 - \frac{4\pi^2 H f^2}{g} + \frac{\pi}{2}\frac{r_w^2}{L^2}\sqrt{\frac{\pi f}{KS_s}}(1+i)\right|^{-1}, \tag{3}$$

where $A(\nu, c)$ is the ratio of the dilatational strain to the vertical ground velocity which is a function of the Poisson's ratio ν and the seismic phase velocity c, Γ is the ratio of the confined aquifer fluid pressure to changes in the dilatational static strain and is inferred from the tidal response [*Rojstaczer and Agnew*, 1989], f is frequency, H is the water column height, and r_w is the well bore radius. The quantity $A(\nu, c)$ is $0.46/c$ for a Rayleigh wave in a Poisson solid [*Ben-Menahem and Singh*, 1981]. We use c = 3.7 km s^{-1} as a representative value for the Rayleigh wave phase velocity at the site. On the basis of records of the 2002 Denali earthquake, the actual frequency-dependent phase velocity could possibly vary by as much as 3.3–4.1 km s^{-1} for 20–35 s Rayleigh waves at this site. The variability in c introduces an error of as much as 10% in χ. More significantly, we expect some coupling between the fluid pressure and the other seismic phases. In fractured rock, shear stresses can produce oscillations in some orientations and Love waves are occasionally observed in this well. However, full prediction of the effects of all the seismic phases requires that we know the full three-dimensional strain tensor at the site. Such an inversion would require a local seismic array, which was not emplaced at the time of the earthquakes studied here. We show below that the overall spectral response and relative changes can be satisfactorily explained with a simplified model in which only the large dilatation of the Rayleigh waves affects the hydrological system. The specific parameters of the response is also consistent with independent measurements from a pumping test. Therefore we accept the simplified model of equation (3) as an adequate representation of the coupling.

2.2. Water Level Steps

[11] The rapid step in water level during the Oaxaca earthquake occurred during the seismic shaking (Figure 4). The water level is recorded independently on both the float and the pressure transducer. Therefore the step in the record was not caused by instrumental error. Even given a 10 min ambiguity in arrival time due to a station clock error (Figure 4), the step must have occurred during the passage of the seismic waves. We use the frequency content of the dispersed Rayleigh wave to align the records more precisely.

[12] The well record for the Oaxaca event shows only small oscillations due to surface waves prior to the step

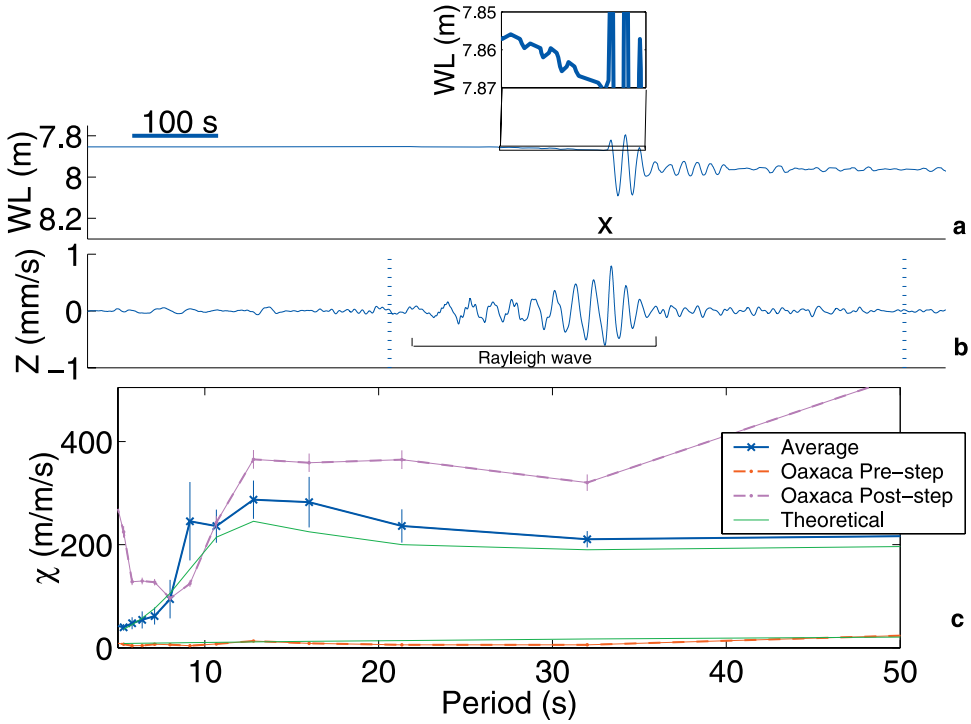

Figure 4. Oaxaca earthquake. (a) Water level measured by float. A timing error results in a 10 min indeterminacy in the arrival time in the well record. The step in the well record at the time indicated by the 'x' may occur at any time between the dashed lines relative to the absolute time in the seismic record. The records are aligned to match the high frequency cycles at the end of the dispersed Rayleigh wave train. The Rayleigh wave propagation time between YBH and the well is 22–29 s, i.e., less than the clock error. No attempt is made to correct for variable phase delays between the seismic station and the well. Inset shows magnified view of water well record before the step. (b) Vertical ground velocity as recorded at YBH. Amplitude is decreased by 6% for geometric spreading and radiation pattern differences between YBH and Grants Pass. The 100 s scale bar from Figure 4a also applies to Figure 4b. (c) Amplification factor χ as a function of period before and after the step for Oaxaca. The theoretical curves are from equation (3) with parameters as in Table 1 except the fracture length L is as annotated. For comparison, the average response from seven earthquakes as shown in Figure 3b is replotted here. Below 20 s, the average response is from the regional data; above 20 s, the average response is from the teleseismic data.

(Figure 4). The float was clearly free to track the water level as tides and random small fluctuations were recorded, yet significant amplification of the Rayleigh wave train did not occur until after the step. More specifically, before the step the amplification factor χ is less than 10 m/(m/s) at 0.06 Hz, whereas after the step χ at 0.06 Hz resumes a nearly normal value of 380 ± 19 m/(m/s) (Figure 4b). Since neither the tidal amplification nor the well geometry changes with time, the change in χ must be due to a local change in K or, more plausibly, the geometry of the fracture. Equation (3) shows that much larger changes in K than L are required to achieve a significant effect. The reduction in χ before the step by a factor of nearly 40 requires at least a 75% reduction in fracture length L if all other parameters in equation (3) are constant (Figure 4). As will be detailed below, a simultaneous change in χ and a step can occur if the seismic waves remove a temporary low permeability barrier in the fracture near the well. Removing the barrier both returns the amplification to normal and allows the well to drain. A local blockage in the fracture has only small effects on the amplitude of the aquifer tidal signal as the long-period tidal stresses sample the average wall rock (matrix) properties.

[13] Drops in water level can be sudden, as in the case of Oaxaca, or gradual, as in the case of Petrolia (Figure 1). The different drop durations correspond to differing distances from the well to localized sources of pore pressure change [*Roeloffs*, 1998]. For times much greater than the duration of the seismic wave train, we model the effect of the pressure step on the well as the one-dimensional solution to a diffusion equation in an unbounded, homogeneous aquifer [*Crank*, 1975]

$$W = W_0 - \frac{\Delta p}{\rho g}\,\mathrm{erfc}\left(d/\sqrt{4Dt}\right), \tag{4}$$

where W is the water level, W_0 is the initial water level, Δp is the amplitude of the pressure drop at the source, d is the distance from the source of the pore pressure change to the fracture, t is the time since the drop at the source, and $D \equiv K/S_s$ is the hydraulic diffusivity [*Freeze and Cherry*, 1979]. On the basis of the pumping test and the seismic wave

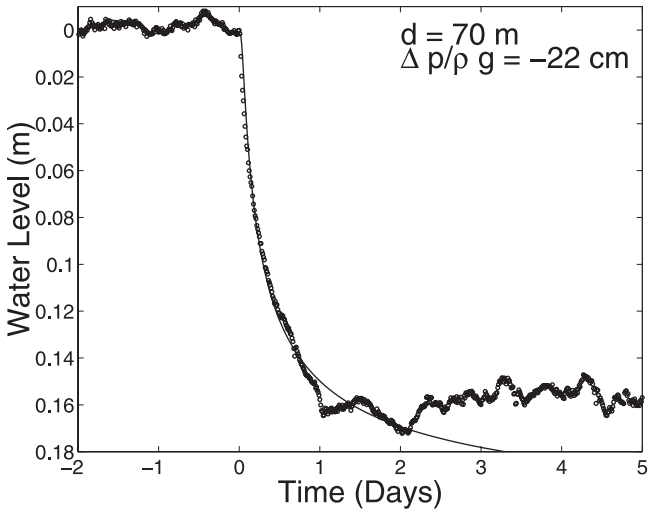

Figure 5. Petrolia earthquake water well record. The data (circles) are the detrended, tidally corrected water level measured below an arbitrary 0 during the Petrolia earthquake (time 0). Smooth curve is a least squares fit of equation (4) to the data for the time of 0–2 days with D = 0.2 m^2 s^{-1}.

response, D in the granodiorite matrix is 0.2 m^2 s^{-1} (Table 1). A least squares fit of the Petrolia water level record to equation (4) yields d = 70 m and $\Delta p/\rho g = -22$ cm (Figure 5). The misfit at large times may be due to unrelated seasonal trends or the flow encountering aquifer boundaries not sampled in the 52 hour pumping test. Unfortunately, there is no other monitored well sampling the same deep, confined aquifer within a 1 km radius; therefore we cannot triangulate to determine a more accurate location for the pressure source.

[14] The process generating the step did not affect χ in the well during the Petrolia earthquake since d greatly exceeds the pressure diffusion length scale for the seismic waves ($\sqrt{D\tau}$ = 2 m, where τ is the dominant wave period of 21 s). For Oaxaca, the drop is a step function to within the data resolution and the solution to the diffusion equation is the trivial one, i.e., d = 0 and $\Delta p/\rho g = -11$ cm. Both steps are consistent with a localized, instantaneous source of pressure. The consistency suggests that the same mechanism is active both near and far from the well, i.e., the steps are not generated by the well bore itself.

3. Mechanism

[15] The static stress change at the well directly generated by the 3850 km distant ($\Delta = 34.65^0$) M_w = 7.4 Oaxaca earthquake is less than 0.2 Pa. A static stress change of 10^3 Pa is required to explain the observed 11 cm water level drop. Therefore we can eliminate static stress as the cause of the drop and limit our investigations to a detailed study of the dynamic stresses (seismic waves).

[16] On the basis of the observations we propose a new model for water level changes in wells far from an earthquake (Figure 6). The permeability structure is dominated by highly conductive fractures. From time to time, these fractures become clogged with weathering products and low permeability flocs of colloidal material. The fluid pressure on the upgradient (or upstream) side of the low-permeability barrier in steady state increases relative to the unclogged state (Figure 6b). In addition, the effective fracture size is smaller and the value of χ measured by an intersecting well is therefore reduced. When a seismic wave passes, it induces rapid flow between the formation and fracture which removes the barrier by loosening particles and entraining them. Once the barrier is removed, water drains from the well to produce a step in pressure as the permeability structure returns to its normal state. If the barrier forms at some distance from the fracture intersected by the well, the pressure change diffuses gradually to the fracture, but if the barrier is immediately adjacent to the fracture, then the observed drop is very rapid.

[17] Water pumped from deep in the aquifer contains 4×10^7 micron-size aluminosilicate particles per liter. These suspended weathering products could aggregate to form the requisite blockages. Dense clay flocs have conductivities comparable to the wall rock value 7×10^{-8} m s^{-1} [*Freeze and Cherry*, 1979] and could thus effectively block the fracture. For simplicity, we assume that the floc and wall rock conductivities are identical and the water flows through both according to Darcy's law,

$$u = -K/(\phi\rho g)\nabla p, \tag{5}$$

where u is the interstitial fluid velocity and ϕ is the porosity. The Darcy (volumetrically average) velocity is ϕu. In order to deposit a 0.3 mm thick barriers of densely packed colloids in two years, we require a Darcy velocity of 5 m d^{-1}. In steady state, the head drop across this barrier is 25 cm (2.5 kPa of pressure). When the barrier is removed, the upgradient side returns to the initial pressure P_0 by dropping by half the head difference, or 13 cm.

[18] The fluid velocity at the edge of the flocs adjacent to the wall is of the same order as that draining the matrix by continuity. The seismic waves induce a flow rate Q_{clog} that is observed during Oaxaca to be 5×10^{-5} m^3 s^{-1} during the Rayleigh waves before the step. If the fracture thickness w is 1 mm and the clogged fracture length L is at most 30 m as inferred from the response (Figure 4), the fluid velocity is Q_{clog}/wL = 1 mm s^{-1}. Viscous stress on the particles is approximately $-\eta u/R$, where η is the viscosity of water (10^{-3} Pa s) and R is the radius of the particle (1 μm). The interstitial fluid velocity u is at least the Darcy velocity, ϕu, and can be substantially greater if ϕ is small. The resulting viscous shear is 1 Pa which is sufficient to initiate motion and disaggregate flocs [*Kessler*, 1993]. Low permeability clay flocs can have very high porosity (>99%), therefore when the flocs are disaggregated, the separated micron-scale clay particles no longer have a significant effect on the permeability [*Kessler*, 1993]. It is possible that the small amplitude solid strains of the shaking also contribute directly to loosening the barriers, but there is no need to invoke such a difficult mechanism as the observed induced flow velocities are sufficient for entrainment.

[19] The gradual Petrolia drop suggests that seismic waves can induce floc-entraining flow velocities outside the immediate vicinity of the well bore. Seismic waves induce pressure gradients between any zones with different values of Γ, i.e., different compressibilities and porosities.

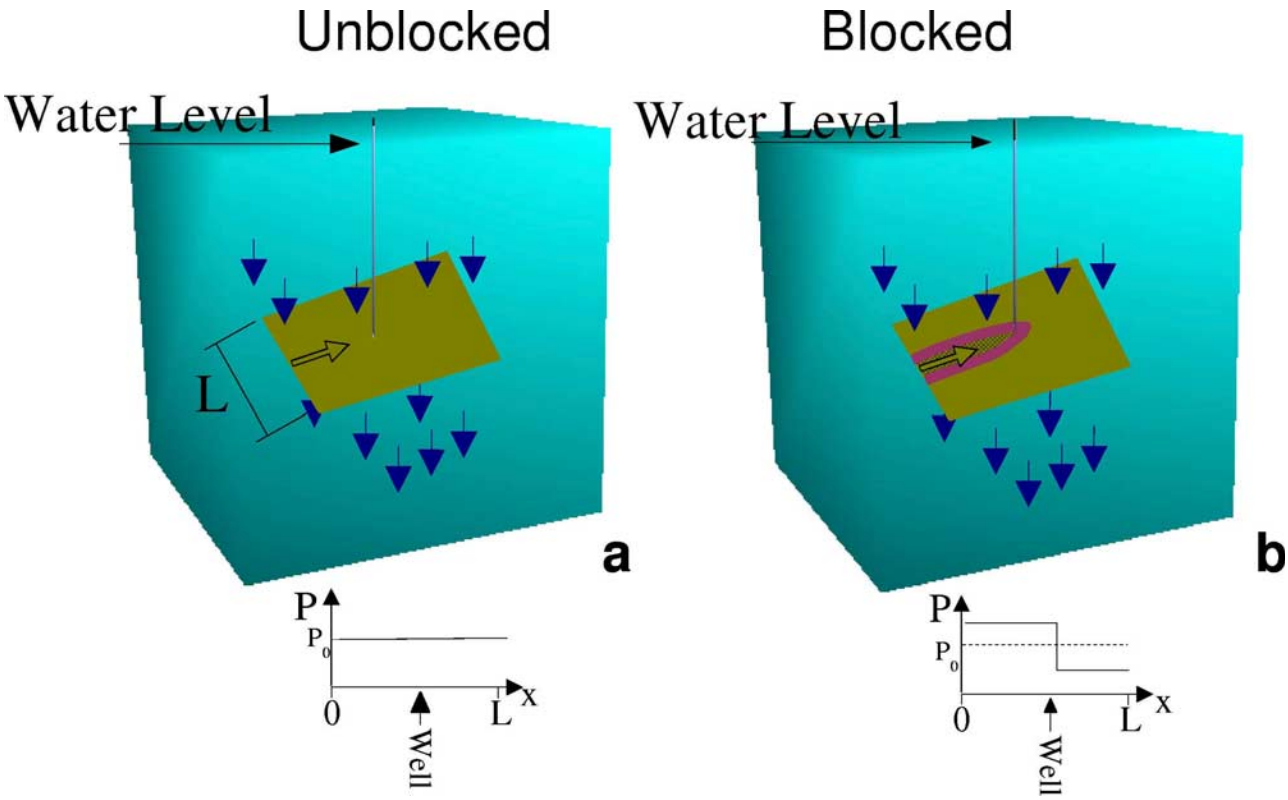

Figure 6. Cartoon of the blockage mechanism. (a) Well in fractured granodiorite system under normal, unclogged conditions. Schematic graph of pressure along the centerline of the fracture as a function of distance x from the upgradient edge. Blue arrows show the flow in the matrix; outlined arrow is the flow inside the fracture. (b) Following the formation of a barrier (red line) the steady state flow has increased pressure on the upgradient side relative to the unclogged state. Initial P_0 from Figure 6a shown for reference. The new effective fracture area (shaded area inside thick red line) is at most $(L/4)^2$.

The head difference between two geological units can be 80% of the head difference between one of the units and the well bore. The pressure difference Δp_{12} between two units with tidal amplifications Γ_1 and Γ_2 in response to a dilatational strain θ is $(1 - \Gamma_2/\Gamma_1)\Gamma_1\theta$. If a well is drilled into the Γ_1 unit, the pressure difference Δp_w between the unit and the well is $\Gamma_1\theta$. Therefore the ratio $\Delta p_{12}/\Delta p_w$ is $(1 - \Gamma_2/\Gamma_1)$. The range of Γ observed in nature is at least a factor of 5 [*Roeloffs*, 1998]. In open fractures, Γ is 1. As long as these contrasts are sustained over sharp boundaries, such as a fracture wall, flow will be on the order of that observed in the well. In a fracture that does not intersect a well, there will be no water column resonance, i.e., the second term of equation (3) will be negligible. The absence of water column resonance far from the well reduces flow velocities by only 40% relative to those observed here.

[20] The Oaxaca earthquake was followed 2 weeks later by shaking with 20% greater vertical ground velocity from the Hector Mine earthquake (Figure 2). No rainfall occurred between the events and all other observables were indistinguishable, yet the second event produced no step. The above model predicts that a barrier could not reform within 2 weeks as the particle concentration is too low. Therefore no step is expected with the second earthquake despite its size.

[21] One observation not directly addressed by the model is that the pressure changes at the well are always drops. An abundant source of weathering material or disequilibrium precipitation may exist downgradient of the well. Alternatively, the fracture may have an easily blocked constriction downgradient. In either case, the downgradient location of the blockage would then favor drops at the well.

[22] Other mechanisms that have been suggested for far-field coseismic pore pressure changes include mobilization of gas bubbles [*Linde et al.*, 1994; *Roeloffs*, 1998; *Sturtevant et al.*, 1996], shaking-induced dilatancy [*Bower and Heaton*, 1978] and fracture of an impermeable fault [*King et al.*, 1999]. The high tidal amplification implies that a compressible gas phase comprises $<10^{-4}$% of the aquifer; therefore bubbles cannot account for the observed water level drop. The other two mechanisms fail to explain the observed drop in effective permeability followed by the return to the original value. Both dilatancy and fracture models predict that the effective permeability, and hence χ, should increase immediately following the earthquake. We observe that the post-step response of Oaxaca is of the same order as the long-term average.

4. The 3 November 2002 M_w = 7.9 Denali Earthquake

[23] While this manuscript was in preparation, another large earthquake generated a coseismic step at NVIP-3. The

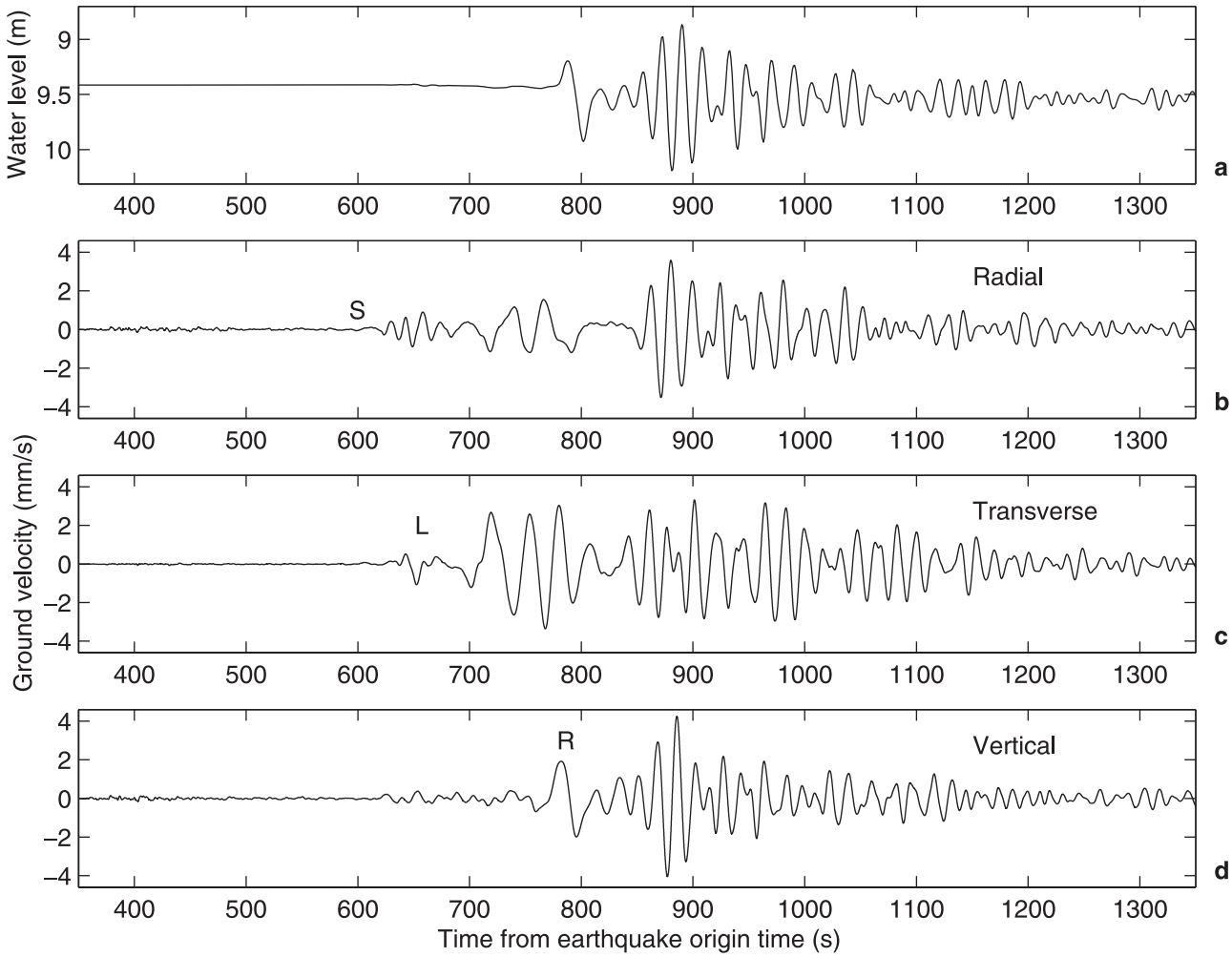

Figure 7. Water level and three-component seismogram for $M_w = 7.9$ Denali earthquake. (a) Water level in the well with 12 cm coseismic step. (b) Radial, (c) transverse, and (d) vertical components of ground velocity. Annotation marks the arrivals of the *S* wave (S), Love wave (L), and Rayleigh wave (R).

3 November 2002 Denali earthquake (Figure 1) allowed us to independently test the model already developed based on the Oaxaca data.

[24] The Denali earthquake ($\Delta = 25.2°$) generated a sudden drop in water level during the shaking (Figure 7). The ambiguity in aligning the seismic and hydrologic records is <5 s. Uncertainties in site effects were eliminated since there was a Streickeisen STS-2 broadband seismometer at the well site beginning in December 2001. Like Oaxaca, the Denali record shows very little response to shaking before the step and a normal response afterward. However, unlike the previous case, the step occurred at the beginning of the Rayleigh wave, therefore the responses before and after cannot be directly compared as in Figure 4c. For Denali, the water level is responding first to the *S* and then to the Rayleigh wave. Shear phase coupling is observed for other earthquakes and is probably due to an anisotropic poroelastic response in the fractured rock [*Wang*, 2000]. The Oaxaca earthquake appears to have been very convenient in that it had a long, dispersed Rayleigh wave which generated a constant excitation with a varying response.

[25] Before the 12 cm step, the peak flow rate was 4×10^{-5} m^{-3} s^{-1}, i.e., nearly identical to the 5×10^{-5}m^3 s^{-1} value of Q_{clog} observed for Oaxaca. The entrainment threshold for Denali is consistent with that proposed for Oaxaca.

[26] The 4 mm s^{-1} shaking of the Denali earthquake is some of the strongest shaking recorded on site. The last earthquake with a normal oscillatory record at the well prior to the Denali event was the 23 June 2001 $M_w = 8.4$ Peru earthquake that produced 17 cm oscillatory motion in the well in response to 0.7 mm s^{-1} shaking (Figure 8). The observation is consistent with the predicted amplitude of 19 ± 2 cm calculated from equation (3) using the unblocked fracture parameters in Table 1. In contrast, the 23 October 2002 $M_w = 6.7$ foreshock to the Denali event shook the Oregon site with an amplitude of 0.04 mm s^{-1}. Although this shaking is smaller than most earthquakes we studied, according to equation (3) with the values in Table 1, the water level should have oscillated with an amplitude of 1 cm. The observed water level was less than the 0.6 mm trigger for high sample rate recording. This order of magnitude suppression of water level shaking is consistent with the

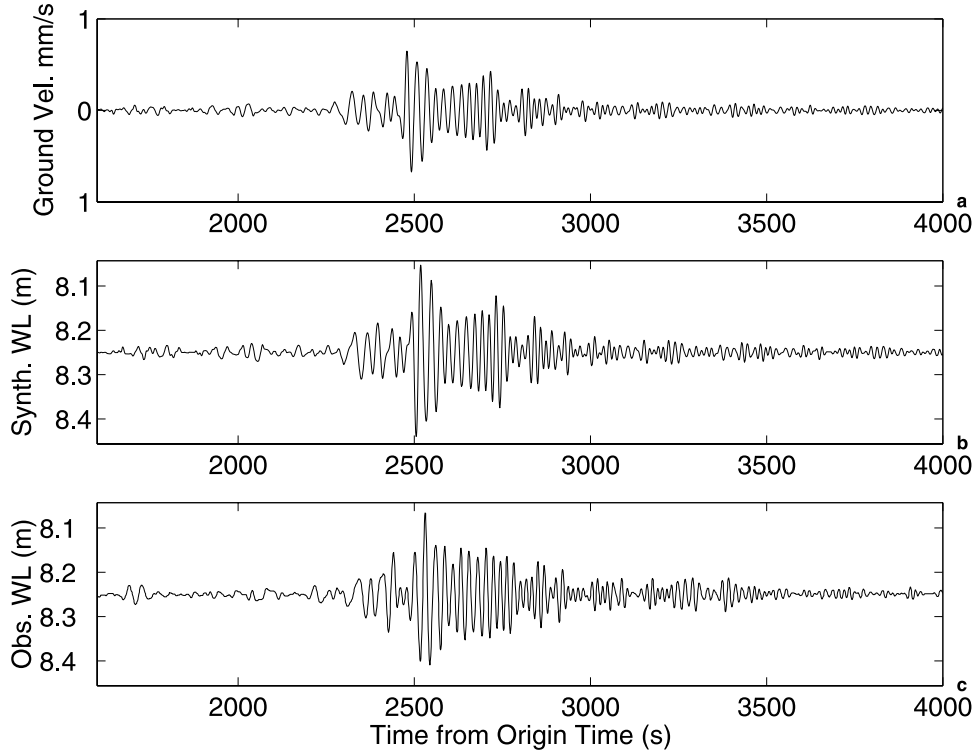

Figure 8. M_w = 8.4 2 June 2001 Peru (Δ = 74.5°) earthquake. (a) Vertical component of ground velocity recorded at YBH with amplitude corrected for geometric spreading between YBH and the well. (b) Synthetic water level recorded computed using the seismogram in Figure 8a, equation (3), and the parameters in Table 1. (c) Observed water level.

barrier model. If the barrier formed over the 1.4 year interval between the Peru and Denali earthquake and all other parameters are the same as in the above model, we predict a 9 cm head drop could occur during barrier removal. This result from our order-of-magnitude model is reasonably near the observed value of 12 cm.

5. Implications for Earthquakes

[27] We have constrained here a naturally occurring process that suddenly redistributes pore pressure on fractures. Faults, like fractures, form hydrological boundaries that have contrasting porosity (storage) with the surrounding rock and can accumulate sediment. Seismically induced pore pressure steps can occur by the mechanism proposed here in any hydrogeological systems that has (1) low matrix specific storage, (2) fractures or faults, and (3) a source of material for clogging. At least one other well-studied site of coseismic steps is in a granitoid pluton with conditions 1–2 documented and condition 3 likely [*King et al.*, 1999].

[28] Recent studies of regional-scale seismic triggering suggest that seismic waves generate pore pressure changes in geothermal areas that in turn generate seismicity [*Hill et al.*, 1993; *Brodsky et al.*, 2000]. Geothermal systems satisfy all three conditions above. In particular, rapid precipitation of minerals is more common in geothermal areas than in ordinary hydrogeologic environments because of the large temperature and chemical gradients [*Lowell et al.*, 1993]. We speculate that high incidences of triggered seismicity have been observed in geothermal systems [*Hill et al.*, 1993; *Brodsky et al.*, 2000; *USGS*, 2000] because of unstable permeability structures generated by hot, circulating fluids. Shaking by seismic waves loosens new precipitate and readjusts the pore pressure on faults and fractures as is observed in the Grants Pass well. The rapid redistribution of pore pressure may promote earthquakes by quickly reducing the effective stress on faults locally. Although the NVIP-3 well records only water level drops, the barrier removal model requires pore pressure increases on the downgradient end of the fracture or fault.

[29] In geothermal areas under typical conditions, precipitation rates can be a factor of 15 greater than modeled for Grants Pass [*Lowell et al.*, 1993] resulting in barrier thicknesses and step amplitudes proportionally larger. If all other factors are equal to what we observe and model above, the pressure change on a fault in a geothermal area will be 4×10^{-2} MPa which is sufficient to trigger an earthquake according to static stress studies [*Hardebeck et al.*, 1998].

6. Conclusions

[30] The water well record from the Oaxaca earthquake presented here is the first high sample rate recording of a rapid far-field coseismic well step ever published to the best of our knowledge. Such records are rare because (1) only a small fraction of wells show far-field coseismic steps and (2) hydrogeologists normally record water level at rates no greater than 2×10^{-3} Hz. We analyzed this unique water well record in conjunction with seismic data to show that

during a rapid drop in water level, as the well drains, the response χ increases from the unusually low value of 9 ± 2 m/(m/s) to a more normal value of 380 ± 19 m/(m/s). We interpret the change as the removal of a temporary blockage in a fracture. Whether or not a step occurs depends on the preexisting hydrogeology as well as the seismic input.

[31] **Acknowledgments.** This work was supported in part by a NSF Earth Science Postdoctoral Fellowship and the Miller Institute for Basic Research. We thank N. Beeler, D. Hill and S. Rojstaczer for reviews of an early form of this manuscript. J. Barker gave insights into interpreting the pumping test data, P. Hsieh advised on flow in fractured rocks and C. Chen contributed SEM imaging of the particulates. Data from Yreka Blue Hill are courtesy Berkeley Digital Seismic Network. PASSCAL instrument center provided the STS-2 seismometer for the 2002 installation.

References

Ben-Menahem, A., and S. J. Singh, *Seismic Waves and Sources*, Dover, Mineola, N. Y., 1981.

Bower, D. R., and K. C. Heaton, Response of an aquifer near Ottawa to tidal forcing and the Alaskan earthquake of 1964, *Can. J. Earth Sci.*, *15*, 331–340, 1978.

Brodsky, E. E., V. Karakostas, and H. Kanamori, A new observation of dynamically triggered regional seismicity: Earthquakes in Greece following the August, 1999 Izmit, Turkey earthquake, *Geophys. Res. Lett.*, *27*, 2741–2744, 2000.

Coble, R., The effects of the Alaskan earthquake of March 27, 1964, on ground water in Iowa, *Proc. Iowa Acad. Sci.*, *72*, 323–332, 1965.

Cooper, H. H., J. D. Bredehoeft, I. S. Papdopulos, and R. R. Bennett, The response of well-aquifer systems to seismic waves, *J. Geophys. Res.*, *70*, 3915–3926, 1965.

Crank, J., *The Mathematics of Diffusion*, Oxford Sci., Oxford, U.K., 1975.

Freeze, R. A., and J. A. Cherry, *Groundwater*, Prentice-Hall, Old Tappan, N. J., 1979.

Gringarten, A. C., and H. J. Ramey, The use of source and Green's functions in solving unstead-flow problems in reservoirs, *Trans. SPE*, *255*, 285–296, 1973.

Hardebeck, J., J. Nazareth, and E. Hauksson, The static stress change triggering model: Constraints from two southern California aftershock sequences, *J. Geophys. Res.*, *103*, 24,427–24,438, 1998.

Hill, D. P., et al., Seismicity remotely triggered by the magnitude 7.3 Landers, California, earthquake, *Science*, *260*, 1617–1623, 1993.

Hsieh, P., J. Bredehoeft, and S. Rojstaczer, Response of well aquifer systems to earth tides: Problem revisted, *Water Res. Res.*, *24*, 468–472, 1988.

Johnston, M. J. S., D. P. Hill, A. T. Linde, J. Langbein, and R. Bilham, Transient deformation during triggered seismicity from the 28 June 1992 M_w = 7.3 Landers earthquake at Long Valley volcanic caldera, California, *Bull. Seismol. Soc. Am.*, *85*, 787–795, 1995.

Kessler, J., Transport and channeling effects in a fracture partially clogged with colloidal material, Ph.D. thesis, Univ. of Calif., Berkeley, 1993.

King, C.-Y., S. Azuma, G. Igarashi, M. Ohno, H. Saito, and H. Wakita, Earthquake-related water-level changes at 16 closely clustered wells in Tono, central Japan, *J. Geophys. Res.*, *104*, 13,073–13,082, 1999.

Linde, A., I. Sacks, M. Johnston, D. Hill, and R. Bilham, Increased pressure from rising bubbles as a mechanism for remotely triggered seismicity, *Nature*, *371*, 408–410, 1994.

Love, A., *Mathematical Theory of Elasticity*, Cambridge Univ. Press, New York, 1927.

Lowell, R., P. VanCappellen, and L. Germanovich, Silica precipitation in fractures and the evolution of permeability in hydrothermal upflow zones, *Science*, *260*, 192–194, 1993.

Matsumoto, N., Regression-analysis for anomalous changes of groundwater level due to earthquakes, *Geophys. Res. Lett.*, *19*, 1193–1196, 1992.

Roeloffs, E., Persistent water level changes in a well near Parkfield, California, due to local and distant earthquakes, *J. Geophys. Res.*, *103*, 869–889, 1998.

Rojstaczer, S., and D. Agnew, The influence of formation material properties on the response of water levels in wells to earth tides and atmospheric loading, *J. Geophys. Res.*, *94*, 12,403–12,411, 1989.

Sturtevant, B., H. Kanamori, and E. E. Brodsky, Seismic triggering by rectified diffusion in geothermal systems, *J. Geophys. Res.*, *101*, 25,269–25,282, 1996.

U.S. Geological Survey, Preliminary report on the 10/16/1999 *M*7.1 Hector Mine, California earthquake, Reston, Va., 2000.

Wang, H., *Theory of Linear Poroelasticity*, Princeton Univ., Princeton, N.J., 2000.

Woodcock, D., and E. Roeloffs, Seismically induced water-level oscillations in a fractured-rock aquifer well near Grants Pass, Oregon, *Oreg. Geol.*, *58*, 27–33, 1996.

E. E. Brodsky, Department of Earth and Space Sciences, University of California, Los Angeles, 1708 Geology Building, 595 Charles Young Drive East, Los Angeles, CA 90095-1567, USA. (brodsky@ess.ucla.edu)

E. Roeloffs, U.S. Geological Survey, 1300 SE Cardinal Court, Building 10, Suite 100, Vancouver, WA 98683, USA. (evelynr@usgs.gov)

D. Woodcock, Oregon Water Resources Department, 158 12th Street NE, Salem, OR 97301, USA. (Douglas.E.Woodcock@wrd.state.or.us)

I. Gall, Oregon Water Resources Department, 942 SW 6th Street, Suite E, Grants Pass, OR 97526, USA. (Ivan.K.Gall@wrd.state.or.us)

M. Manga, Department of Earth and Planetary Sciences, University of California, 307 McCone Hall, Berkeley, CA 94720-4767, USA. (manga@seismo.berkeley.edu)